

Recent progress on the QCD phase diagram

More precision in a smaller volume

Jana N. Guenther

September 12th 2024



Motivation for a small volume

- It saves computational time:
 - fewer lattice points
 - less noise on derivatives
 - often reduces overlap problem in reweighing methods
- Investigation of transitions requires finite volume scan
- Heavy ion collisions take place in a finite volume (though it is not clear, how to translate to the lattice)
- Point of interest for DSE ([Bernhardt:2022mnx], [Bernhardt:2021iql])

1 Fluctuations in the Continuum [Borsanyi:2023wno]

- State of the art
- Our set-up and analysis
- Results

2 Critically from fluctuations

- Lee-Yang zeros and pad[Please insert into preamble] approximations
- Results

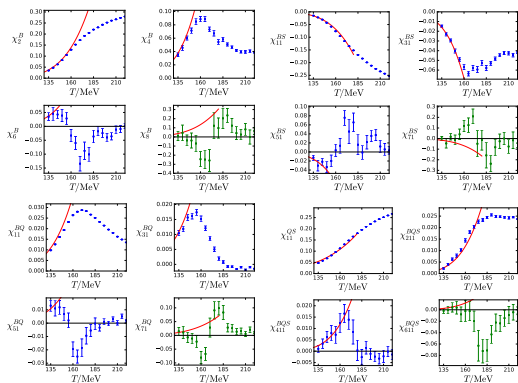
3 Observerbles taylored to small voulme [Borsanyi:2024dro]

Fluctuations on the lattice

$$\chi_{i,j,k}^{B,Q,S} = \frac{\partial^{i+j+k}(p/T^4)}{(\partial\hat{\mu}_B)^i(\partial\hat{\mu}_Q)^j(\partial\hat{\mu}_S)^k}, \quad \hat{\mu}_i = \frac{\mu}{T}$$

Today:

$$\chi_i^B = \frac{\partial^i(p/T^4)}{(\partial\hat{\mu}_B)^i}$$



[Borsanyi:2018grb]

State of the art

1 Fluctuations in the Continuum [Borsanyi:2023wno]

- State of the art
- Our set-up and analysis
- Results

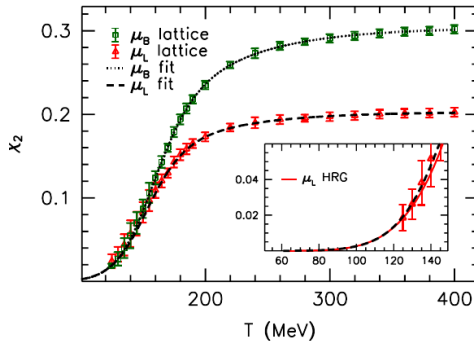
2 Critically from fluctuations

- Lee-Yang zeros and pad[Please insert intopreamble] approximations
- Results

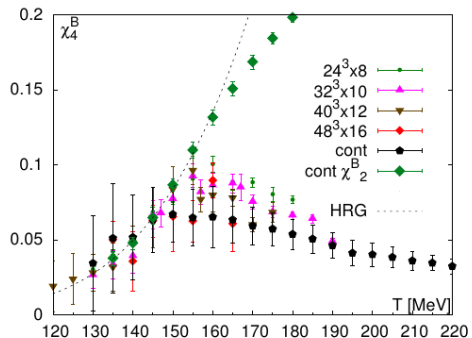
3 Observerbles taylored to small voulme [Borsanyi:2024dro]

State of the art

χ_2^B and χ_4^B in the continuum



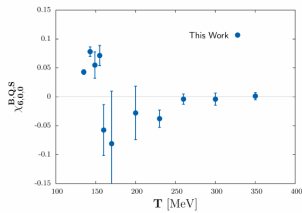
[Borsanyi:2012cr]



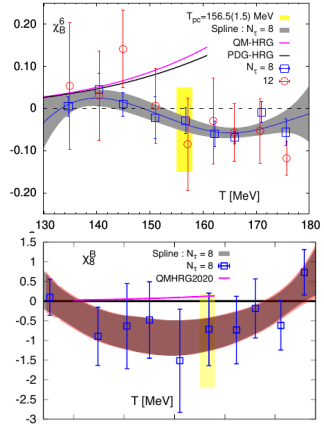
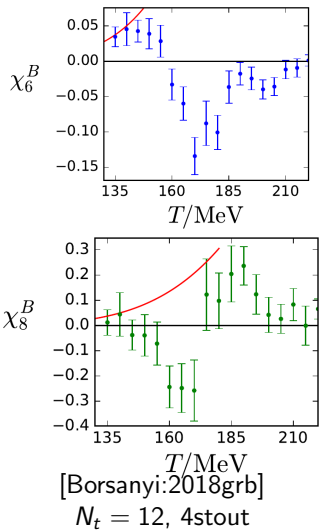
[Bellwied:2015lba]

State of the art

χ_6^B and χ_8^B on finite lattices

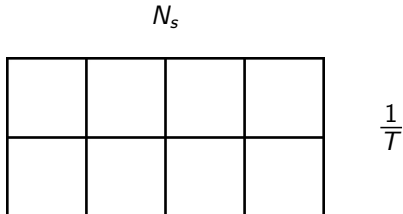


[DElia:2016jqh]
 $N_t = 6$, 2stout



State of the art

The continuum limit

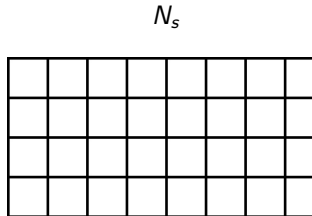


$$\frac{1}{T}$$



State of the art

The continuum limit

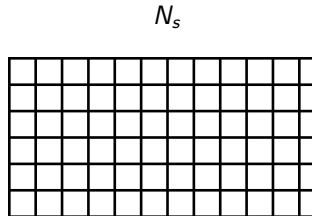


$$\frac{1}{T}$$



State of the art

The continuum limit

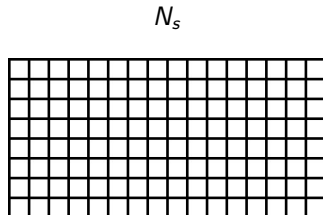


$$\frac{1}{T}$$



State of the art

The continuum limit

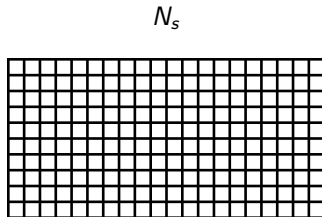


$$\frac{1}{T}$$



State of the art

The continuum limit



$\frac{1}{T}$



State of the art

The continuum limit

 N_s

$\frac{1}{T}$



Our set-up and analysis

1 Fluctuations in the Continuum [Borsanyi:2023wno]

- State of the art
- **Our set-up and analysis**
- Results

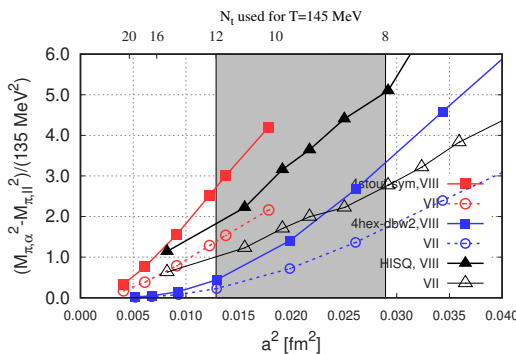
2 Critically from fluctuations

- Lee-Yang zeros and pad[Please insert into preamble] approximations
- Results

3 Observerbles taylored to small voulme [Borsanyi:2024dro]

Our set-up and analysis

Lattice set-up



- 4Hex + dbw2 action
- lattices: $16^3 \times 8, 20^3 \times 10, 24^3 \times 12$
- $\mu_S = 0$
- scale setting with f_π and w_1
- Exponential definition of the chemical potential (introduced like a constant imaginary gauge field) → derivatives with respect to the chemical potential can be shown to be UV finite by virtue of a $U(1)$ symmetry [Hasenfratz:1983ba]

Our set-up and analysis

Systematic errors

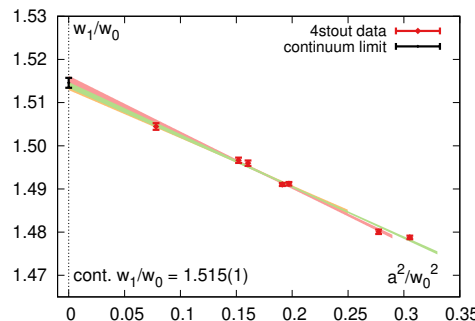
We have to deal with systematic errors from the continuum extrapolation and the scale setting.

Our set-up and analysis

Systematic errors

We have to deal with systematic errors from the continuum extrapolation and the scale setting.
Scale setting is done with f_π and w_1 .

$$W(t)|_{t=w_1^2} = 0.7 , W(t) \equiv t \frac{d}{dt} \{ t^2 \langle E(t) \rangle \}$$



Our set-up and analysis

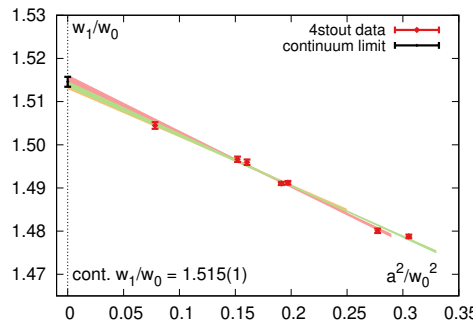
Systematic errors

We have to deal with systematic errors from the continuum extrapolation and the scale setting.
 Scale setting is done with f_π and w_1 .

Continuum extrapolation:

$$W(t)|_{t=w_1^2} = 0.7 , W(t) \equiv t \frac{d}{dt} \{ t^2 \langle E(t) \rangle \}$$

$$\hat{O}(T, 1/N_\tau^2) = \sum_{i=1}^M \left(\alpha_i + \beta_i \frac{1}{N_\tau^2} \right) s_i(T) ,$$



s_i : set of basis spline function. We take three different sets of node points.

Our set-up and analysis

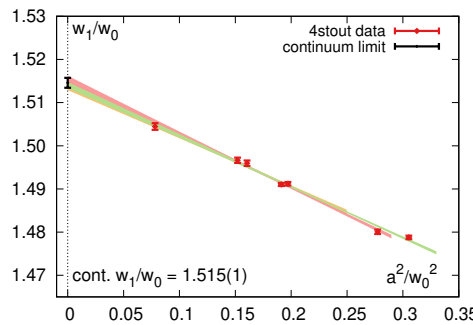
Systematic errors

We have to deal with systematic errors from the continuum extrapolation and the scale setting.
 Scale setting is done with f_π and w_1 .

Continuum extrapolation:

$$W(t)|_{t=w_1^2} = 0.7 , W(t) \equiv t \frac{d}{dt} \{ t^2 \langle E(t) \rangle \}$$

$$\hat{O}(T, 1/N_\tau^2) = \sum_{i=1}^M \left(\alpha_i + \beta_i \frac{1}{N_\tau^2} \right) s_i(T) ,$$



s_i : set of basis spline function. We take three different sets of node points.

The final results are obtained by combining the $6 = 2 \times 3$ analyses to construct a histogram.

1 Fluctuations in the Continuum [Borsanyi:2023wno]

- State of the art
- Our set-up and analysis
- Results

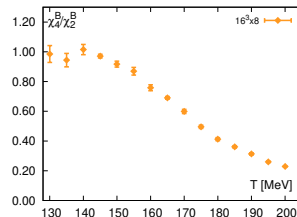
2 Critically from fluctuations

- Lee-Yang zeros and pad[Please insert intopreamble] approximations
- Results

3 Observerbles taylored to small voulme [Borsanyi:2024dro]

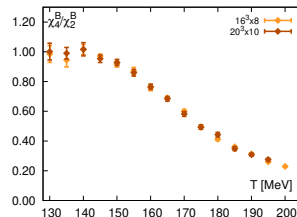
Results

New continuum results



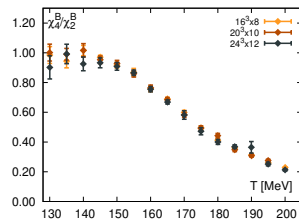
Results

New continuum results



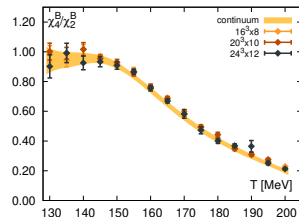
Results

New continuum results



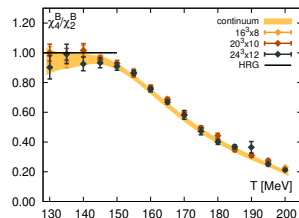
Results

New continuum results



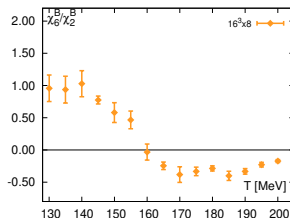
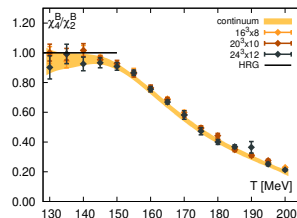
Results

New continuum results



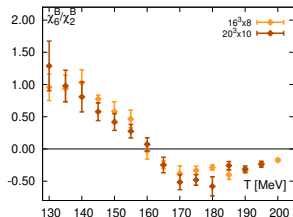
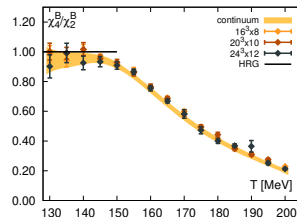
Results

New continuum results



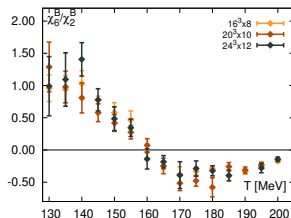
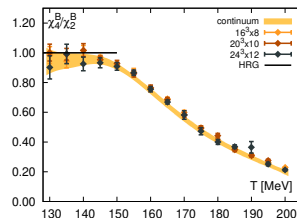
Results

New continuum results



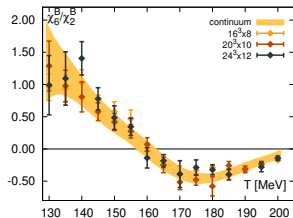
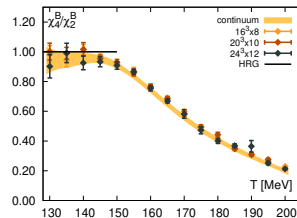
Results

New continuum results



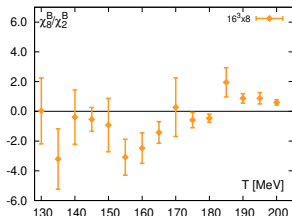
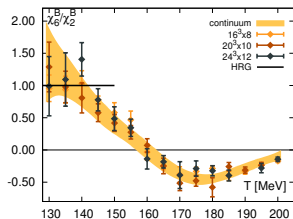
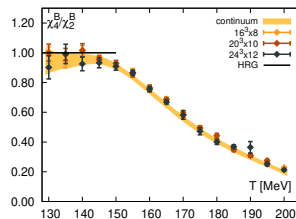
Results

New continuum results



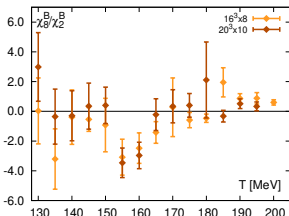
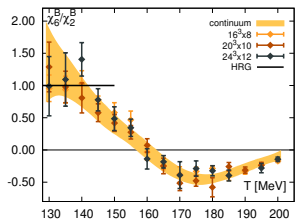
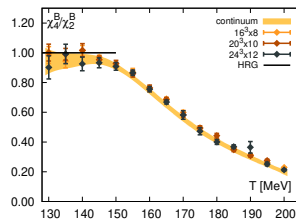
Results

New continuum results



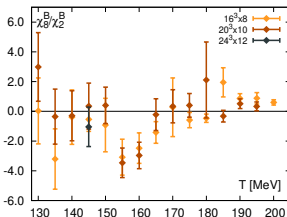
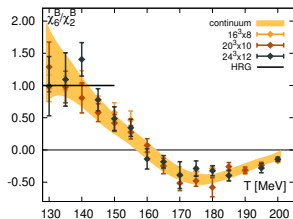
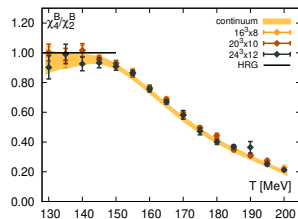
Results

New continuum results



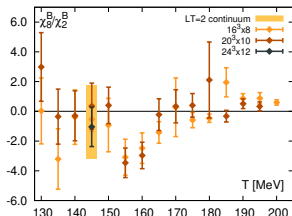
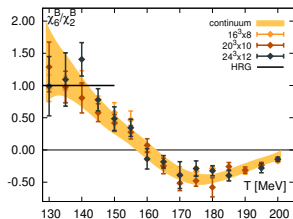
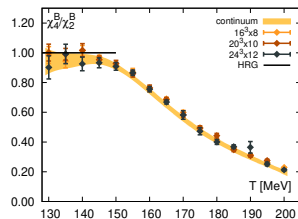
Results

New continuum results



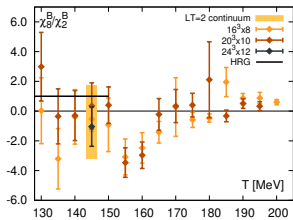
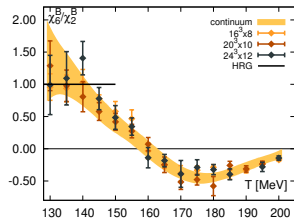
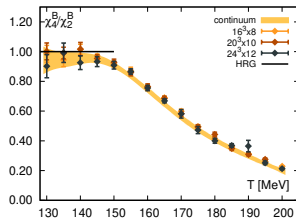
Results

New continuum results



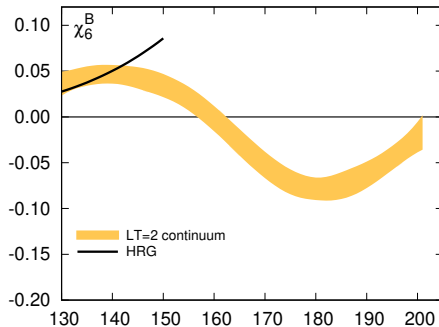
Results

New continuum results



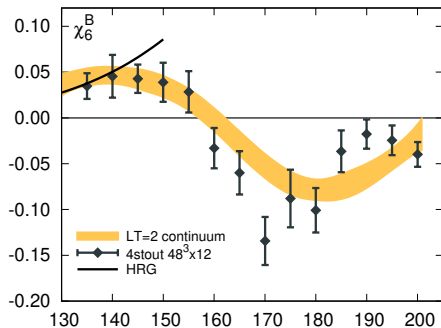
Results

Comparision with different actions



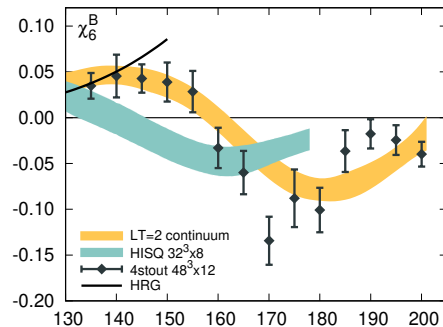
Results

Comparision with different actions



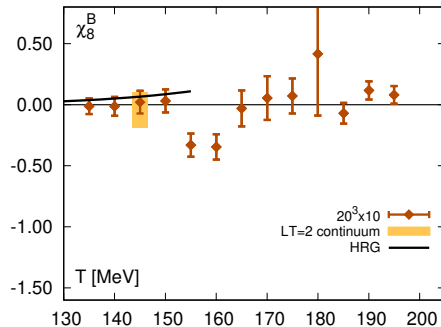
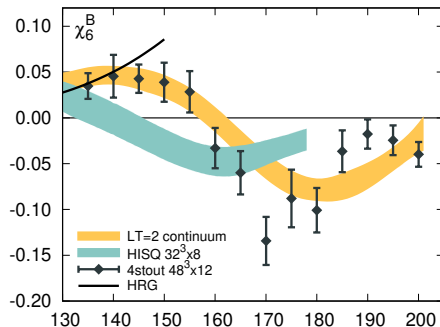
Results

Comparision with different actions



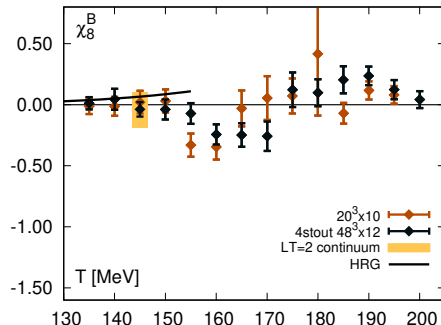
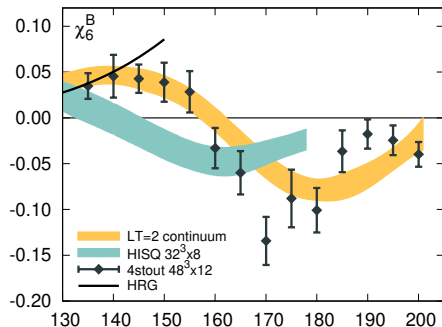
Results

Comparision with different actions



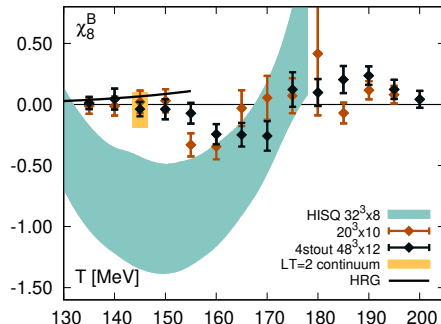
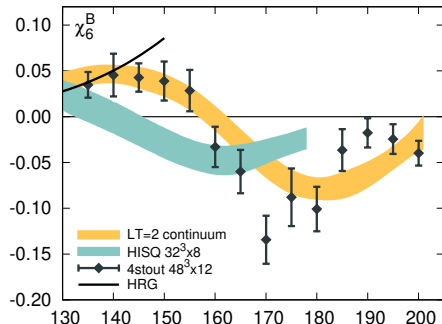
Results

Comparision with different actions

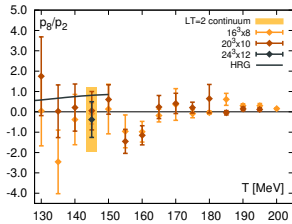
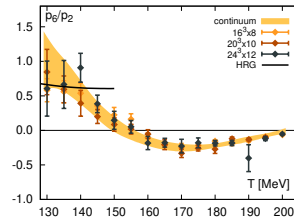
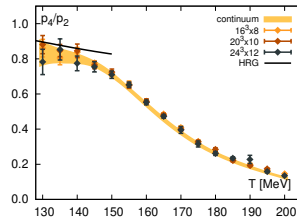


Results

Comparision with different actions

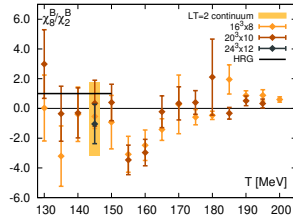
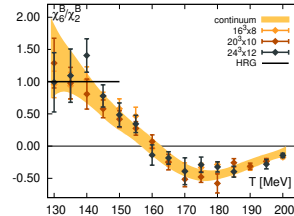
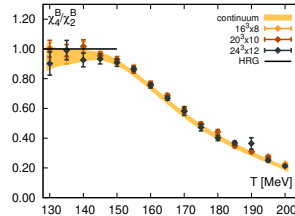
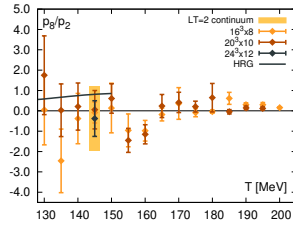
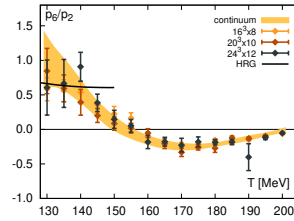
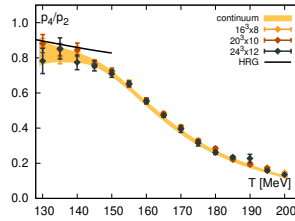


Results

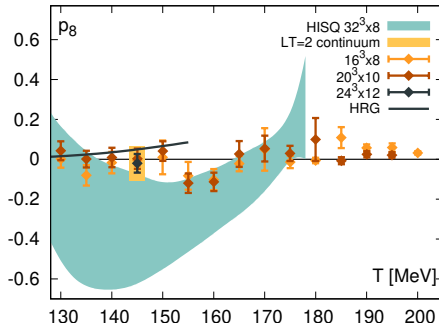
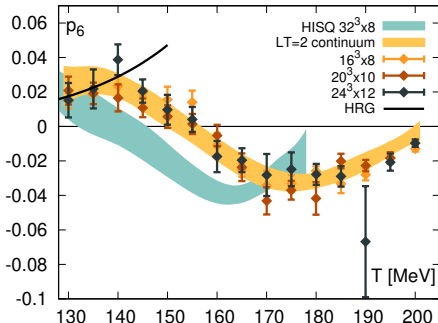
Strangeness neutrality: $\langle n_S \rangle = 0$ – Continuum results

Results

Strangeness neutrality: $\langle n_S \rangle = 0$ – Continuum results

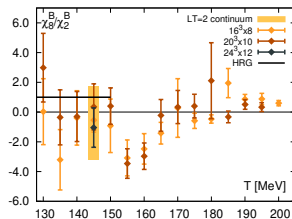
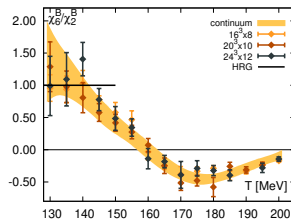
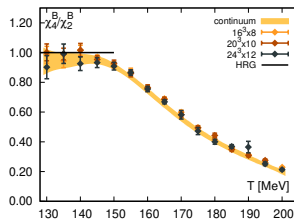


Results

Strangeness neutrality: $\langle n_S \rangle = 0$ –Comparision with different actions

Results

Conclusion



- First continuum extrapolated results for high order baryon number fluctuations
- A 4Hex + dbw2 action allowed for a continuum limit from $N_t = 8, 10, 12$
- With $LT = 2$ the volume effects are under control in the low temperature region.

1 Fluctuations in the Continuum [Borsanyi:2023wno]

- State of the art
- Our set-up and analysis
- Results

2 Critically from fluctuations

- Lee-Yang zeros and pad[Please insert into preamble] approximations
- Results

3 Observerbles taylored to small voulme [Borsanyi:2024dro]

Lee-Yang zeros and padé approximations

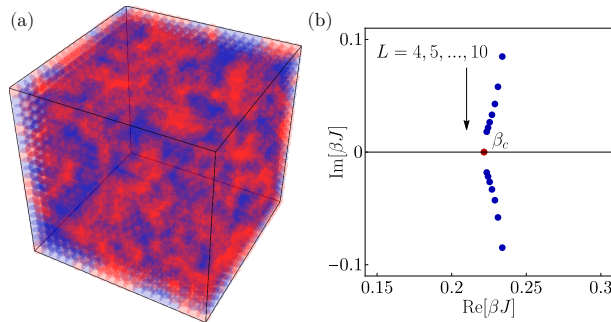
Lee-Yang

- Lee-Yang zeros (LYZ) and Lee-Yang edge singularity [Lee,Yang'59]

Lee-Yang zeros and padé approximations

Lee-Yang

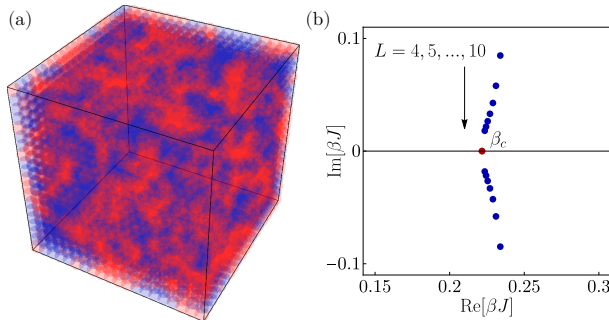
- Lee-Yang zeros (LYZ) and Lee-Yang edge singularity [Lee,Yang'59]
- This has been studies in the same universality class [arXiv:1905.02379]



Lee-Yang zeros and padé approximations

Lee-Yang

- Lee-Yang zeros (LYZ) and Lee-Yang edge singularity [Lee, Yang'59]
- This has been studies in the same universality class [arXiv:1905.02379]



- a small excerpt of other work by others:
 - Parma Bielefeld [2405.10196]
 - Simran Singh PhD Thesis
 - Gökçe Başar [2312.06952]
 - Giordano, Pásztor [1904.01974]
 - Mukherjee, Skokov [1909.04639]
 - Wakayama et al. [1802.02014]

Lee-Yang zeros and padé approximations

What we work with

- To access zeros of Z , we can look at $\log(Z) = p$
- Written as a Taylor series

$$\Delta p = \frac{p(T, \mu_B) - p(T, 0)}{T^4} = \sum_{n=0} \frac{\chi_{2n}(T)}{(2n)!} \left(\frac{\mu_B}{T}\right)^{2n} \quad \chi_n = \frac{\partial^n(p/T^4)}{(\partial\mu/T)^2}$$

- χ_{2n} is given by simulations at $\mu_B = 0$
- These coefficients can be used in conjunction with a scaling relation for extrapolation
- In addition we can model:

$$\chi_1(T, \mu_B) = \sum_{n=1} \frac{\chi_{2n}(T)}{(2n-1)!} \left(\frac{\mu_B}{T}\right)^{2n+1} \quad \chi_2(T, \mu_B) = \sum_{n=0} \frac{\chi_{2n+2}(T)}{(2n)!} \left(\frac{\mu_B}{T}\right)^{2n}$$

Lee-Yang zeros and padé approximations

$$\text{Pade}[m, n] : \frac{P_m(x)}{1+Q_n(x)} = \frac{\sum_{i=0}^m a_i x^i}{1+\sum_{i=1}^n b_i x^i}$$

Lee-Yang zeros and padé approximations

$$\text{Pade}[m, n] : \frac{P_m(x)}{1+Q_n(x)} = \frac{\sum_{i=0}^m a_i x^i}{1+\sum_{i=1}^n b_i x^i}$$

- Convert by solving algebraically: $P_m(x) = T_l(x)(1 + Q_n(x))$ with $T_l(x) = \sum_{i=0}^l c_i x^i$

Lee-Yang zeros and padé approximations

$$\text{Pade}[m, n] : \frac{P_m(x)}{1+Q_n(x)} = \frac{\sum_{i=0}^m a_i x^i}{1+\sum_{i=1}^n b_i x^i}$$

- Convert by solving algebraically: $P_m(x) = T_l(x)(1 + Q_n(x))$ with $T_l(x) = \sum_{i=0}^l c_i x^i$
- solving the equation $1 + Q_n(x) \stackrel{!}{=} 0$ gives the Poles

Lee-Yang zeros and padé approximations

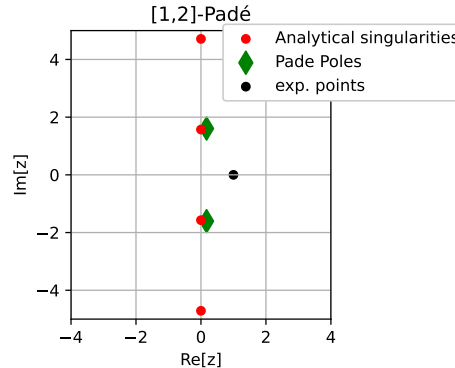
$$\text{Pade}[m, n] : \frac{P_m(x)}{1+Q_n(x)} = \frac{\sum_{i=0}^m a_i x^i}{1+\sum_{i=1}^n b_i x^i}$$

- Convert by solving algebraically: $P_m(x) = T_l(x)(1 + Q_n(x))$ with $T_l(x) = \sum_{i=0}^l c_i x^i$
- solving the equation $1 + Q_n(x) \stackrel{!}{=} 0$ gives the Poles
- Example using $1/\cosh(z)$

Lee-Yang zeros and padé approximations

$$\text{Pade}[m, n] : \frac{P_m(x)}{1+Q_n(x)} = \frac{\sum_{i=0}^m a_i x^i}{1+\sum_{i=1}^n b_i x^i}$$

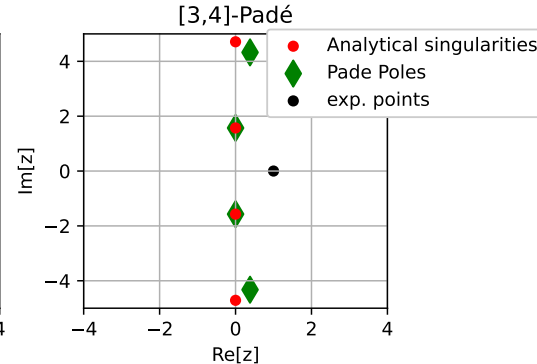
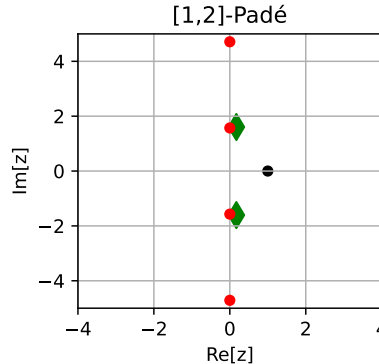
- Convert by solving algebraically: $P_m(x) = T_l(x)(1 + Q_n(x))$ with $T_l(x) = \sum_{i=0}^l c_i x^i$
- solving the equation $1 + Q_n(x) \stackrel{!}{=} 0$ gives the Poles
- Example using $1/\cosh(z)$



Lee-Yang zeros and padé approximations

$$\text{Padé}[m, n] : \frac{P_m(x)}{1+Q_n(x)} = \frac{\sum_{i=0}^m a_i x^i}{1+\sum_{i=1}^n b_i x^i}$$

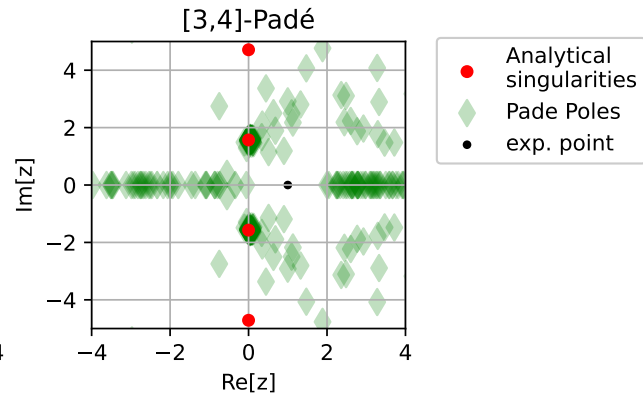
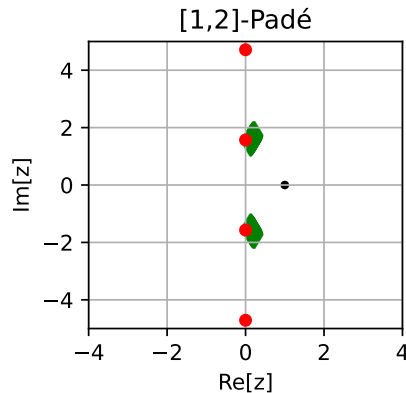
- Convert by solving algebraically: $P_m(x) = T_l(x)(1 + Q_n(x))$ with $T_l(x) = \sum_{i=0}^l c_i x^i$
- solving the equation $1 + Q_n(x) \stackrel{!}{=} 0$ gives the Poles
- Example using $1/\cosh(z)$



Lee-Yang zeros and padé approximations

Padé with Noise

- Adding 3% of noise to each of the derivatives of $1/\cosh(z)$:



Results

1 Fluctuations in the Continuum [Borsanyi:2023wno]

- State of the art
- Our set-up and analysis
- Results

2 Critically from fluctuations

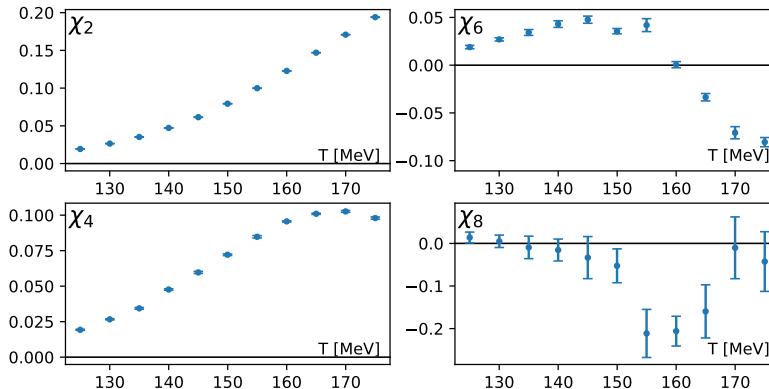
- Lee-Yang zeros and pad[Please insert into preamble] approximations
- Results

3 Observerbles taylored to small voulme [Borsanyi:2024dro]

Results

Lattice Setup

- Volume : $16^3 \times 8$
- $\mathcal{O}(5 \cdot 10^5)$ configurations per T
- 4 HEX smearing
- Simulated at physical quark mass



Results

Analysis:

- $\chi_2, \chi_4, \chi_6, \chi_8 \implies [1, 2]\text{-Pad\'e in } \mu^2$

Results

Analysis:

- $\chi_2, \chi_4, \chi_6, \chi_8 \implies [1, 2]\text{-Pad\'e in } \mu^2$

$$f(T) = \frac{a_1 + a_2\mu^2}{1 + b_1\mu^2 + b_2\mu^4}$$

Results

Analysis:

- $\chi_2, \chi_4, \chi_6, \chi_8 \Rightarrow [1, 2]\text{-Padé in } \mu^2$

$$f(T) = \frac{a_1 + a_2\mu^2}{1 + b_1\mu^2 + b_2\mu^4}$$

- Poles:

$$1 + b_1\mu^2 + b_2\mu^4 \stackrel{!}{=} 0$$

Results

Analysis:

- $\chi_2, \chi_4, \chi_6, \chi_8 \Rightarrow [1, 2]\text{-Pad\'e in } \mu^2$

$$f(T) = \frac{a_1 + a_2\mu^2}{1 + b_1\mu^2 + b_2\mu^4}$$

- Poles:

$$1 + b_1\mu^2 + b_2\mu^4 \stackrel{!}{=} 0$$

- Repeat for each jackknife sample and independently for each temperature.

Results

Analysis:

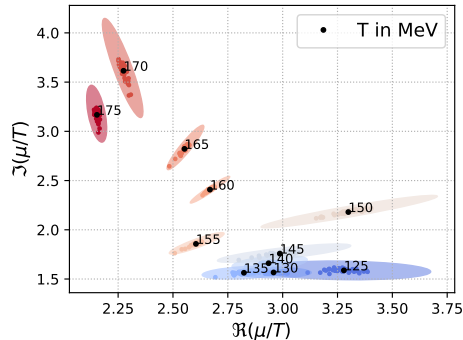
- $\chi_2, \chi_4, \chi_6, \chi_8 \Rightarrow [1, 2]\text{-Padé in } \mu^2$

$$f(T) = \frac{a_1 + a_2\mu^2}{1 + b_1\mu^2 + b_2\mu^4}$$

- Poles:

$$1 + b_1\mu^2 + b_2\mu^4 \stackrel{!}{=} 0$$

- Repeat for each jackknife sample and independently for each temperature.



modeling χ_2

Results

Analysis:

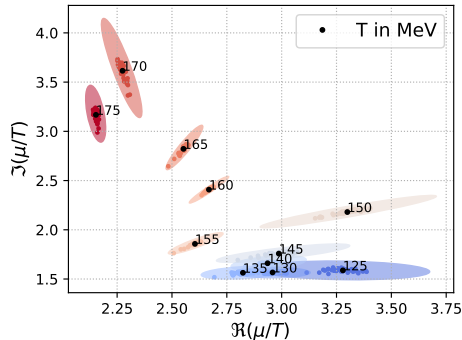
- $\chi_2, \chi_4, \chi_6, \chi_8 \Rightarrow [1, 2]\text{-Padé in } \mu^2$

$$f(T) = \frac{a_1 + a_2\mu^2}{1 + b_1\mu^2 + b_2\mu^4}$$

- Poles:

$$1 + b_1\mu^2 + b_2\mu^4 \stackrel{!}{=} 0$$

- Repeat for each jackknife sample and independently for each temperature.
- Extrapolate T_c , via eg.
 $\text{Im}[\mu_B] = \kappa (\Delta T)^{\beta\delta}$



modeling χ_2

Results

Analysis:

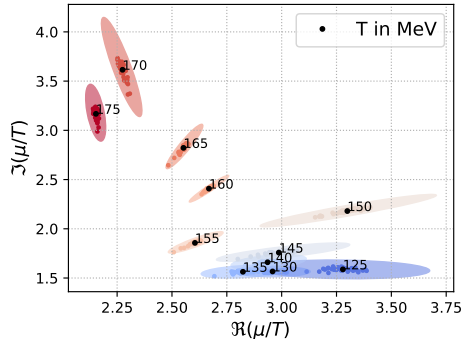
- $\chi_2, \chi_4, \chi_6, \chi_8 \Rightarrow [1, 2]\text{-Padé in } \mu^2$

$$f(T) = \frac{a_1 + a_2\mu^2}{1 + b_1\mu^2 + b_2\mu^4}$$

- Poles:

$$1 + b_1\mu^2 + b_2\mu^4 \stackrel{!}{=} 0$$

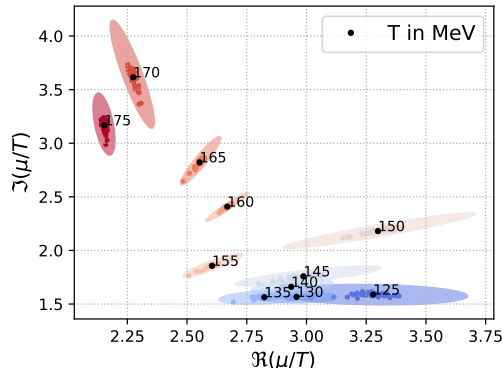
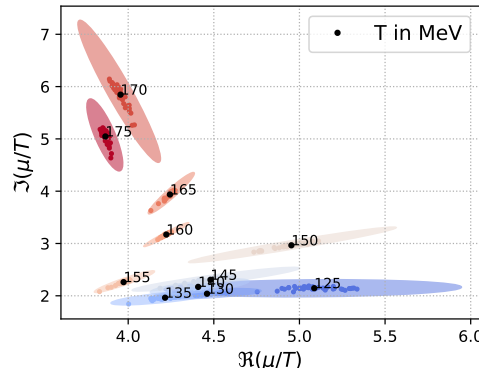
- Repeat for each jackknife sample and independently for each temperature.
- Extrapolate T_c , via eg.
 $\text{Im}[\mu_B] = \kappa (\Delta T)^{\beta\delta}$
- Estimate systematic effects
 - Use Δp or χ_1 or χ_2
 - Vary fit range in temperature
 - Use different scaling ansatz



modeling χ_2

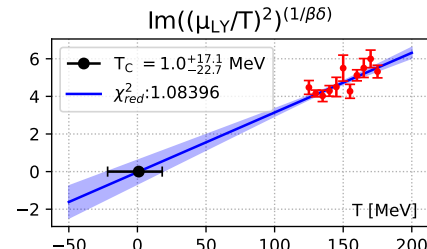
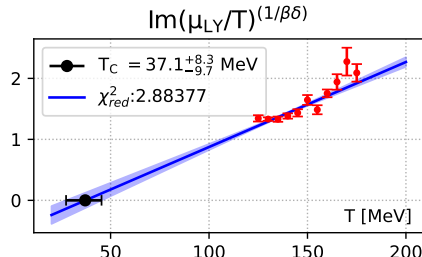
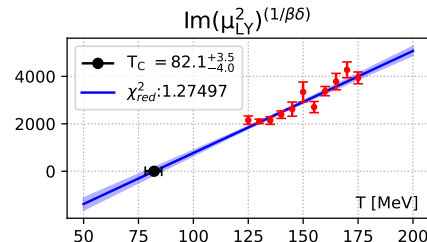
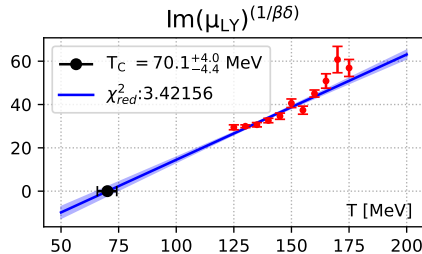
Results

Varying the approximated function

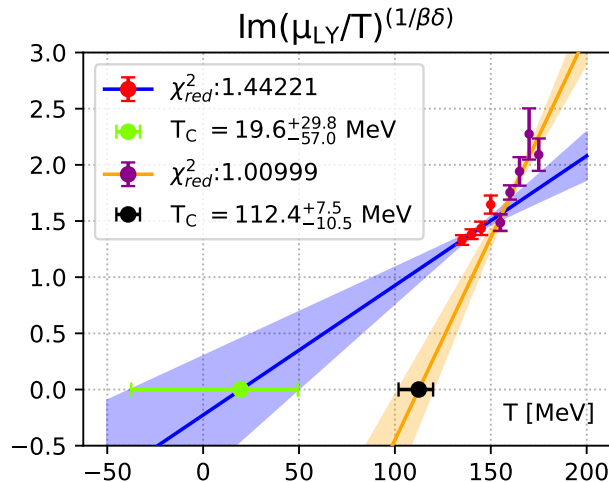
modeling χ_2 modeling $p - p_0$

Results

Varying the scaling variable for $\chi_2 : \kappa \Delta T = \text{Im}(x)^{1/\beta\delta}$



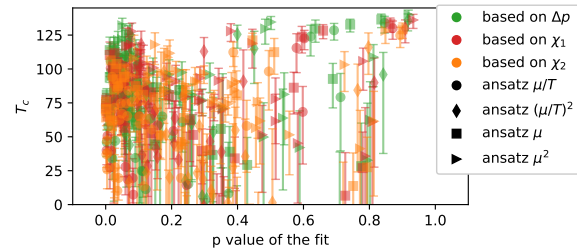
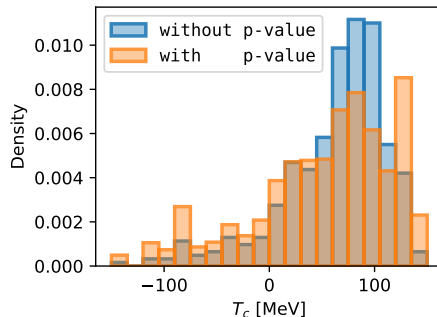
Results

Varying the fit range for χ_2 

Results

Combination

Based on $3[\Delta p, \chi_1, \chi_2] \times 4\left[\mu, \mu^2, \frac{\mu}{T}, \frac{\mu^2}{T^2}\right] \times 36$ Temp. ranges = 432 Fits



Results

Conclusion

- We used a high statistics campaign to look for the Lang Yee Zeros
 - We can estimate T_c with a reasonable statistical error but a high systematic error
 - No systematic control of the Padé order
 - Approximation from a great distance requires strong assumptions
-
- Reliable prediction of the CEP with LYZ from the lattice data requires great care and consideration

1 Fluctuations in the Continuum [Borsanyi:2023wno]

- State of the art
- Our set-up and analysis
- Results

2 Critically from fluctuations

- Lee-Yang zeros and pad[Please insert into preamble] approximations
- Results

3 Observerbles taylored to small voulme [Borsanyi:2024dro]

Properties of QCD crossover

Chiral

- $SU(2) \times SU(2)$ symmetry in the limit
 $m_q \rightarrow 0$
- order parameter: chiral condensate $\langle \bar{\psi}\psi \rangle$
- we study the chiral condensate and its derivative the chiral susceptibility χ

Properties of QCD crossover

Chiral

- $SU(2) \times SU(2)$ symmetry in the limit $m_q \rightarrow 0$
- order parameter: chiral condensate $\langle \bar{\psi} \psi \rangle$
- we study the chiral condensate and its derivative the chiral susceptibility χ

Deconfinement

- Z_3 symmetry in the limit $m_q \rightarrow \infty$
- order parameter: Polykov loop $P \sim e^{-F_Q/T}$
- we study: derived from P the static quark free energy F_Q and the static quark entropy S_Q

Properties of QCD crossover

Chiral

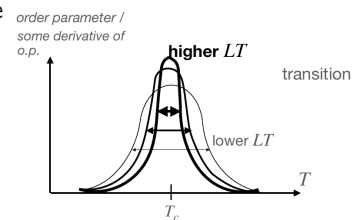
- $SU(2) \times SU(2)$ symmetry in the limit $m_q \rightarrow 0$
- order parameter: chiral condensate $\langle \bar{\psi} \psi \rangle$
- we study the chiral condensate and its derivative the chiral susceptibility χ

We aim to investigate the volume dependence of T_c and the strength of the transition for $\mu_B > 0$ for different definitions

- $m_q \neq 0, \infty \rightarrow$ both only approximate order parameters
- Lattice \rightarrow true transitions do not happen in a finite volume
- how do **chiral** and **deconfinement** observables behave in the limit $LT \rightarrow \infty$

Deconfinement

- Z_3 symmetry in the limit $m_q \rightarrow \infty$
- order parameter: Polykov loop $P \sim e^{-F_Q/T}$
- we study: derived from P the static quark free energy F_Q and the static quark entropy S_Q

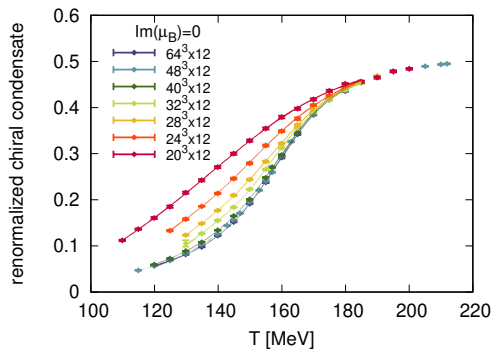


Lattice set-up

- tree-level Symanzik improved gauge action
- $N_f = 2 + 1 + 1$ staggered fermions with 4 stout smearing
- $N_t = 12$, $N_s = 20, 24, 28, 32, 40, 48, 64$
- For $N_s = 32, 40, 48$ simulations also at $\frac{\mu_B^I \pi}{8T} = 3, 4, 5, 6, 6.5, 7$
- strangeness neutrality setting $\langle n_S \rangle = 0$

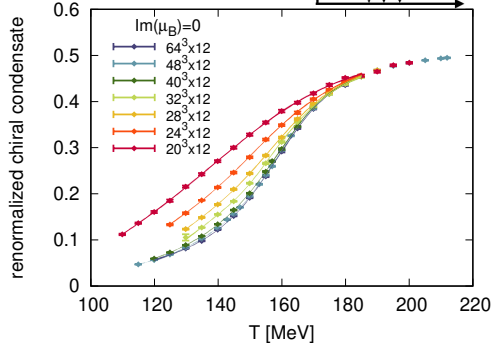
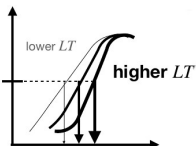
Chiral observables

$$\langle \bar{\psi} \psi \rangle = \frac{T}{V} \frac{\partial \log Z}{\partial m_{ud}}$$



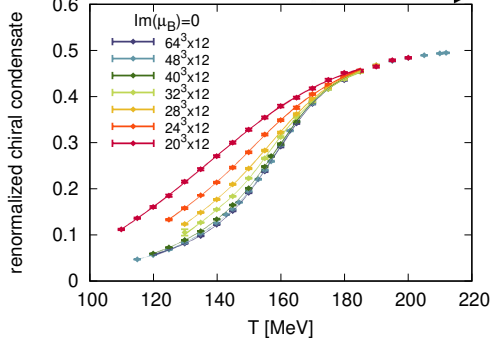
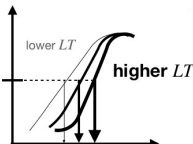
Chiral observables

$$\langle \bar{\psi} \psi \rangle = \frac{T}{V} \frac{\partial \log Z}{\partial m_{ud}}$$

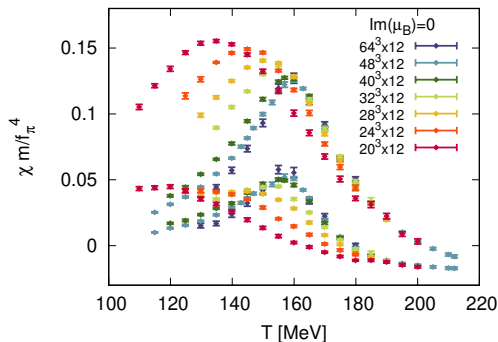


Chiral observables

$$\langle \bar{\psi} \psi \rangle = \frac{T}{V} \frac{\partial \log Z}{\partial m_{ud}}$$

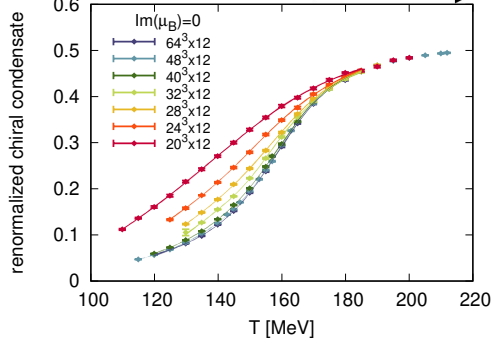
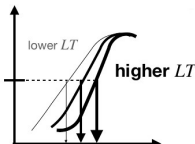


$$\chi = \frac{T}{V} \frac{\partial^2 \log Z}{\partial^2 m_{ud}}, \quad \chi_{\text{disc}} = \left. \frac{T}{V} \frac{\partial^2 \log Z}{\partial m_u \partial m_d} \right|_{m_u=m_d}$$

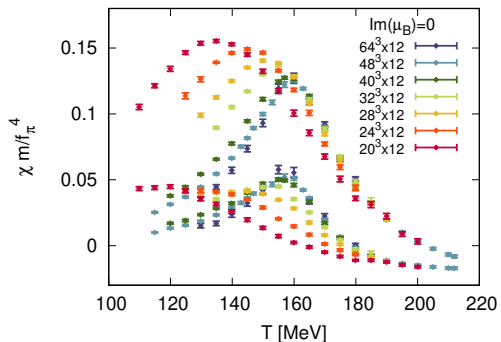


Chiral observables

$$\langle \bar{\psi} \psi \rangle = \frac{T}{V} \frac{\partial \log Z}{\partial m_{ud}}$$



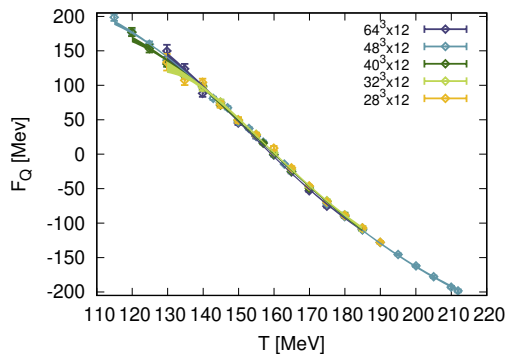
$$\chi = \frac{T}{V} \frac{\partial^2 \log Z}{\partial^2 m_{ud}}, \quad \chi_{\text{disc}} = \left. \frac{T}{V} \frac{\partial^2 \log Z}{\partial m_u \partial m_d} \right|_{m_u=m_d}$$



T_c increases with the volume

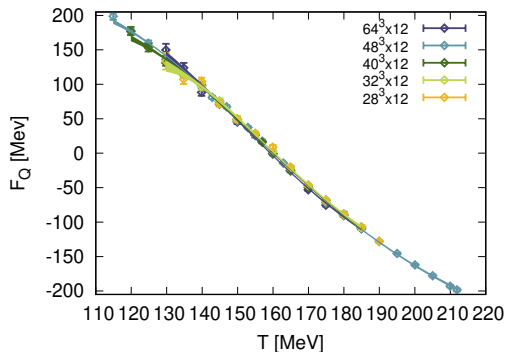
Deconfinement observables

$$F_Q = -T \log \left(\frac{1}{V} |\langle \sum_{\vec{x}} P(\vec{x}) \rangle_T| \right)$$

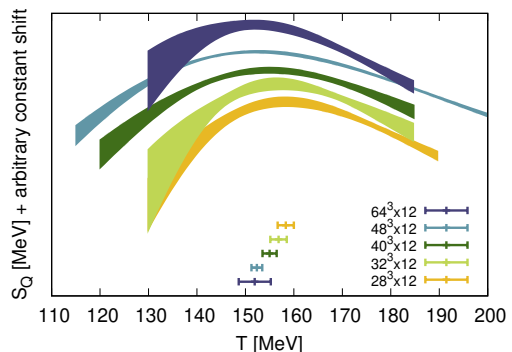


Deconfinement observables

$$F_Q = -T \log \left(\frac{1}{V} \left| \langle \sum_{\vec{x}} P(\vec{x}) \rangle_T \right| \right)$$

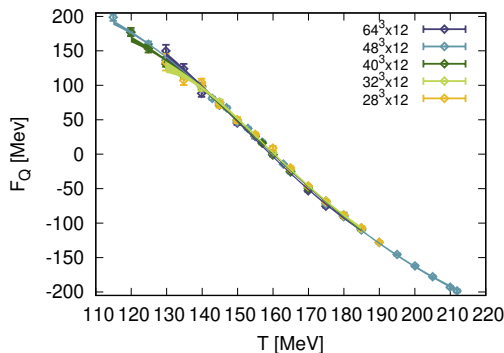


$$S_Q = -\frac{\partial F_Q}{\partial T}$$

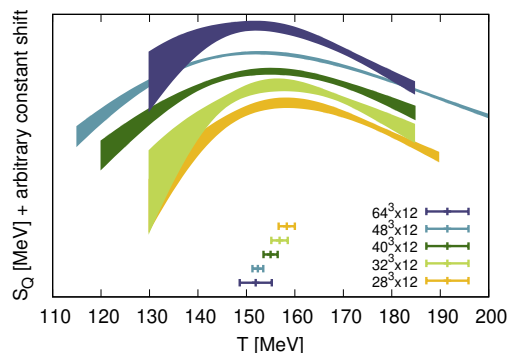


Deconfinement observables

$$F_Q = -T \log \left(\frac{1}{V} \left| \langle \sum_{\vec{x}} P(\vec{x}) \rangle_T \right| \right)$$

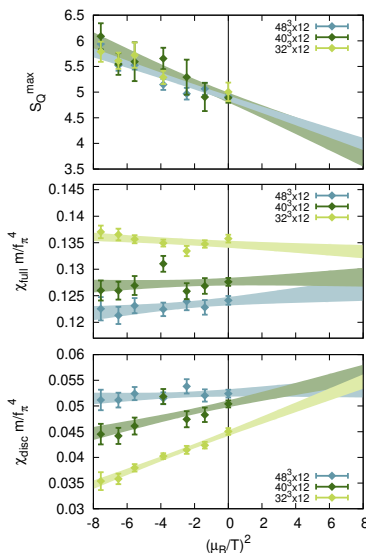


$$S_Q = -\frac{\partial F_Q}{\partial T}$$



Here volume effects are milder then for the chiral observables.

$\mu_B > 0$: Height of peaks of χ , χ_{disc} , S_Q

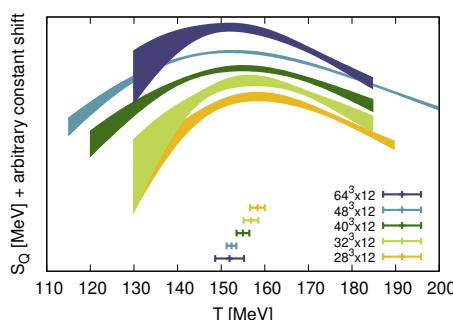
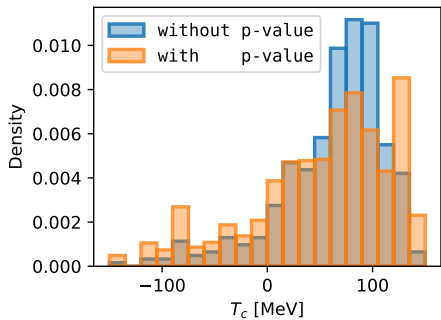
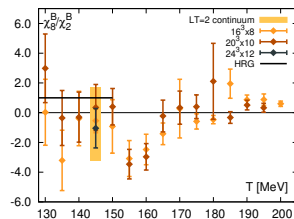
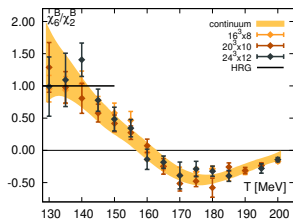
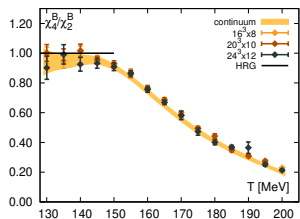


- A rise of the peak hight, could indicate a strengthening of the transition
- This only happens for χ_{disc} , but seems to decrease with volume
- S_Q only has very mild volume effects

Conclusion

- In the thermodynamic limit $T_c^{(S_Q)} < T_c^{(\chi_{\text{disc}})} < T_c^{(\chi)}$
- The volume dependence of T_c depends on the definition
- The **deconfinement** observables we investigated have a milder volume dependence than the **chiral** ones.
- Only the peak of χ_{disc} increases with μ_B

Summary



T [MeV]	$16^3 \times 8$	$20^3 \times 10$	$24^3 \times 12$
130	31741	71090	68689
135	33528	106403	66960
140	34977	69690	75229
145	336975	188571	111435
150	65374	108481	81590
155	34057	96985	89559
160	37145	68619	94053
165	156044	67668	98744
170	34397	42314	11831
175	34180	36522	12089
180	30594	25229	12727
185	30951	18396	13066
190	30293	18267	7141
195	31276	15008	7199
200	31919	13346	7390

Table: Number of configurations analyzed on our three lattice geometries.